Neurobiology of Disease 130 (2019) 104522

Contents lists available at ScienceDirect

Neurobiology of Disease

journal homepage: www.elsevier.com/locate/ynbdi

Deep brain stimulation for Parkinson's disease modulates high-frequency evoked and spontaneous neural activity

Nicholas C. Sinclair[a,b,*], Hugh J. McDermott[a,b], James B. Fallon[a,b], Thushara Perera[a,b], Peter Brown[c], Kristian J. Bulluss[a,d,e], Wesley Thevathasan[a,f,g]

[a] Bionics Institute, Melbourne, Australia
[b] Department of Medical Bionics, The University of Melbourne, Melbourne, Australia
[c] Medical Research Council Brain Network Dynamics Unit, and Nuffield Department of Clinical Neurosciences, University of Oxford, Oxford, United Kingdom
[d] Department of Neurosurgery, St Vincent's and Austin Hospitals, Melbourne, Australia
[e] Department of Surgery, The University of Melbourne, Heidelberg, Australia
[f] Department of Neurology, The Royal Melbourne and Austin Hospitals, Melbourne, Australia
[g] Department of Medicine, The University of Melbourne, Parkville, Australia

ARTICLE INFO

Keywords:
Deep brain stimulation
Parkinson's disease
Evoked resonant neural activity
Local field potentials
High frequency oscillations
Subthalamic nucleus

ABSTRACT

Deep brain stimulation is an established therapy for Parkinson's disease; however, its effectiveness is hindered by limited understanding of therapeutic mechanisms and the lack of a robust feedback signal for tailoring stimulation. We recently reported that subthalamic nucleus deep brain stimulation evokes a neural response resembling a decaying high-frequency (200-500 Hz) oscillation that typically has a duration of at least 10 ms and is localizable to the dorsal sub-region. As the morphology of this response suggests a propensity for the underlying neural circuitry to oscillate at a particular frequency, we have named it evoked resonant neural activity. Here, we determine whether this evoked activity is modulated by therapeutic stimulation – a critical attribute of a feedback signal. Furthermore, we investigated whether any related changes occurred in spontaneous local field potentials. Evoked and spontaneous neural activity was intraoperatively recorded from 19 subthalamic nuclei in patients with Parkinson's disease. Recordings were obtained before therapeutic stimulation and during 130 Hz stimulation at increasing amplitudes (0.67–3.38 mA), 'washout' of therapeutic effects, and non-therapeutic 20 Hz stimulation. Therapeutic efficacy was assessed using clinical bradykinesia and rigidity scores. The frequency and amplitude of evoked resonant neural activity varied with the level of 130 Hz stimulation ($p < .001$). This modulation coincided with improvement in bradykinesia and rigidity ($p < .001$), and correlated with spontaneous beta band suppression ($p < .001$). Evoked neural activity occupied a similar frequency band to spontaneous high-frequency oscillations (200-400 Hz), both of which decreased to around twice the 130 Hz stimulation rate. Non-therapeutic stimulation at 20 Hz evoked, but did not modulate, resonant activity. These results indicate that therapeutic deep brain stimulation alters the frequency of evoked and spontaneous oscillations recorded in the subthalamic nucleus that are likely generated by loops within the cortico-basal ganglia-thalamo-cortical network. Evoked resonant neural activity therefore has potential as a tool for providing insight into brain network function and has key attributes of a dynamic feedback signal for optimizing therapy.

1. Introduction

Deep brain stimulation (DBS) can be a remarkably effective treatment for Parkinson's disease (Diamond and Jankovic, 2005; Montgomery Jr, 2016; Okun, 2012); however, its mechanisms of action are inadequately understood (Herrington et al., 2015; McIntyre and Hahn, 2010; Montgomery and Gale, 2008; Wichmann and DeLong, 2016), making empirical approaches to applying therapy necessary. Stimulation settings are chosen heuristically, reliant on the clinician's experience and observations of immediate changes in clinical signs, which can be a laborious and sometimes intractable process prone to suboptimal outcomes. Furthermore, DBS devices are 'open-loop',

Abbreviations: DBS, deep brain stimulation; STN, subthalamic nucleus; ERNA, evoked resonant neural activity; HFO, high frequency oscillations; UPDRS, Unified Parkinson's disease rating scale; RMS, root mean square.

* Corresponding author at: Bionics Institute, 384-388 Albert St, East Melbourne, Victoria 3002, Australia.
E-mail address: nsinclair@bionicsinstitute.org (N.C. Sinclair).

https://doi.org/10.1016/j.nbd.2019.104522
Received 16 April 2019; Received in revised form 11 June 2019; Accepted 1 July 2019
Available online 02 July 2019

whereby ongoing stimulation is applied using predefined settings regardless of the patient's actual real-time needs. As symptoms fluctuate over both short and long timescales (Little et al., 2013; Marsden et al., 1982), predefined therapy can at times be detrimentally insufficient or excessive. Accordingly, the development of next-generation devices that automate setting selection and autonomously adapt therapy according to patient needs (Little and Brown, 2012; Little et al., 2013; Priori et al., 2013) could revolutionize the efficacy and therefore uptake of DBS. However, these innovations require a robust feedback signal that is reflective of patient state and therapeutic effects.

Hitherto, the search for feedback signals for tailoring DBS therapy has predominantly focused on spontaneous neural activity, including single-unit activity (Rosin et al., 2011), beta-band activity (Arlotti et al., 2016; Little and Brown, 2012; Little et al., 2013; Neumann et al., 2016; Priori et al., 2013), and gamma-band activity (Swann et al., 2018). Coupling between the phase and amplitude of beta- and gamma-band activity has also been proposed as a potential feedback signal (de Hemptinne et al., 2013; López-Azcárate et al., 2010; Özkurt et al., 2011; van Wijk et al., 2016). However, the small and noisy amplitude of such spontaneous activity makes it technically challenging to record with sufficient fidelity in fully implantable devices (Neumann et al., 2016; Stanslaski et al., 2012). Recently, we identified an evoked response recordable from DBS electrodes that may provide an alternative feedback signal and new insights into therapeutic mechanisms (Sinclair et al., 2018). This large amplitude response resembles a decaying oscillation following DBS pulses (e.g. Fig. 1) applied in the vicinity of the subthalamic nucleus (STN). As this suggests the underlying neural circuitry has a tendency to oscillate at a particular frequency, it has been termed evoked resonant neural activity (ERNA).

We reported that ERNA varies across the STN, having largest amplitude in the dorsal region where DBS usually has greatest benefit for Parkinson's disease (Herzog et al., 2004), is absent in neighboring brain regions, and that electrodes recording larger ERNA yield better therapeutic responses to DBS (Sinclair et al., 2018). These findings indicate that ERNA is a clinically relevant signal and not a specious artefact of the recording system. ERNA was also observed to narrow and intensify over a short burst of consecutive pulses (e.g. Fig. 1B), suggesting it could be modulated by DBS. However, whether ERNA is modulated by therapeutically effective DBS – a crucial attribute of a feedback signal for adjusting therapy – is unknown. ERNA also has potential as a tool for investigating oscillations occurring within neural circuits, including any related spontaneous neural activity.

Here, we intraoperatively recorded evoked and spontaneous neural activity from 19 STN in patients with Parkinson's disease. Recordings were obtained before, during and after therapeutic stimulation and compared with non-therapeutic 20 Hz stimulation. Changes in the frequency and amplitude of ERNA were compared across different stimulation levels and with spontaneous local field potentials in the beta (13-30 Hz) and high frequency oscillation (HFO) (200–400 Hz) bands.

2. Material and methods

2.1. Subjects and surgery

Subjects included in this study were patients with Parkinson's disease undergoing scheduled DBS implantation surgery in the awake state after prerequisite screening. Following ethics approval, 10 patients with Parkinson's disease were recruited at St Vincent's Private Hospital (R0236-15) and the Austin Hospital (SSA/15/Austin/266). Due to experimental piloting, in some subjects only a subset of experiments was performed, as indicated in Table 1 along with cohort demographics. In accordance with the Declaration of Helsinki, informed consent was obtained from all subjects after the nature and possible consequences of the study were explained. The study was registered at www.anzctr.org.au (trial # ACTRN12615001368527).

All subjects were implanted with DBS devices by the same surgical team (neurosurgeon K.J.B. and neurologist W.T.) using the same technique. In accordance with their standard clinical practice, electrode arrays (model 3387, Medtronic, Minnesota, USA) were implanted bilaterally using trajectories intended to position electrodes above the

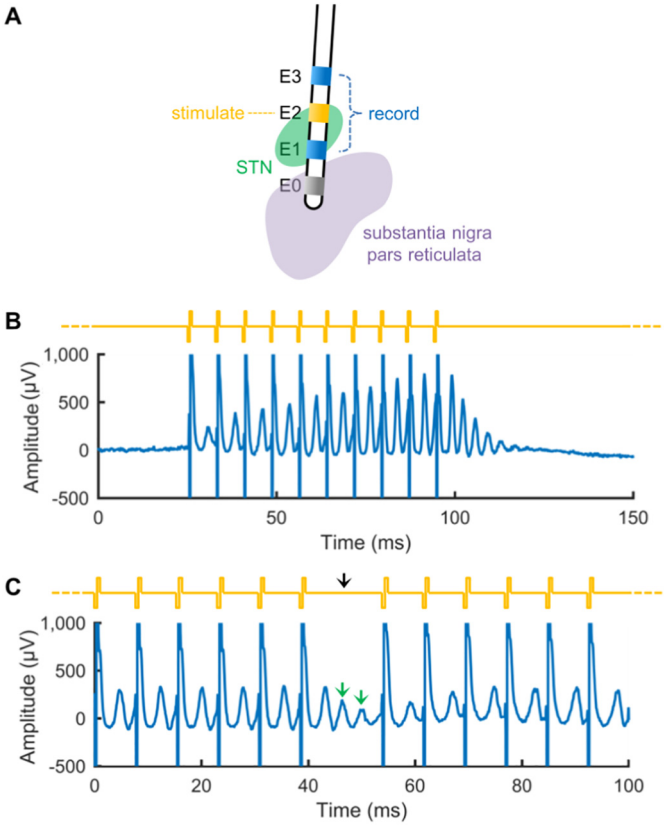

Fig. 1. Stimulation patterns used to measure evoked resonant neural activity (ERNA). (A) Schematic illustration of the targeted electrode positions. Stimulation was applied to E2, which was targeted at the dorsal region of the subthalamic nucleus (STN). Monopolar recordings were re-referenced to a bipolar montage across the stimulating electrode (E1-E3). (B) Burst of ten 130 Hz pulses used as a non-therapeutic 'probe' to elicit ERNA (yellow trace: stimulation waveform). (C) Periodically omitting one pulse per second in otherwise continuous 130 Hz stimulation allowed multiple peaks to be observed during 'clinical' DBS (yellow trace: stimulation waveform; black arrow: omitted pulse; green arrows: additional ERNA peaks observable). (For interpretation of the references to color in this figure legend, the reader is referred to the web version of this article.)

Table 1
Subject demographics and stimulation applied.

Subject	Age	Gender	DBS indication	DBS target	STN tested	Stimulation applied		
						Probe	Clinical	20 Hz
PD03	64	F	MF	STN	L,R	Y	Y	N
PD04	63	M	MF	STN	L*	Y	Y	N
PD05	64	M	MF	STN	L,R	Y	Y	N
PD06	73	F	MF	STN	L,R	Y	Y	N
PD07	61	M	MF	STN	L,R	Y	Y	Y
PD08	65	F	MF	STN	L,R	Y	Y	Y
PD09	54	M	MF	STN	L,R	Y	Y	Y
PD10	55	F	MF	STN	L,R	Y	Y	Y
PD11	62	M	MF	STN	L,R	Y	Y	Y
PD12	66	M	MF, T	STN	L,R	Y	Y	Y

MF: Motor fluctuation, T: Tremor, STN: Subthalamic nucleus, L: Left, R: Right. PD01–02 were pilot experiments in which patterned stimulation was not applied and were excluded from this study. *Only one hemisphere tested due to subject fatigue.

STN (E3, Fig. 1A), within dorsal (E2) and ventral STN (E1), and within the substantia nigra pars reticulata (E0).

Targeting was performed using a CRW (Integra, New Jersey, USA) stereotactic frame with a preoperative three-dimensional volumetric MRI fused to a contrast-enhanced stereotactic CT scan. Micro-electrode recordings were performed to define the location and span of the STN and entry into the substantia nigra pars reticulata, followed by clinical assessments of stimulation induced motor benefit and side effects. When necessary, further single-pass trajectories were explored before a satisfactory trajectory was accepted. Following implantation of both STN, experiments were performed while the subjects remained awake on the operating table with the electrode arrays connected to the recording/stimulation equipment via twist-lock cables (Medtronic, Minnesota, USA). The head frame was then removed and the pulse generator implanted under general anesthesia.

2.2. Stimulation and recordings

Evoked and spontaneous neural activity were recorded under several conditions: 1) prior to therapeutic stimulation ('pre-DBS'), 2) during 130 Hz stimulation progressively increased to therapeutic levels, 3) as therapeutic effects washed out after 130 Hz DBS was stopped ('post-DBS'), and 4) during non-therapeutic 20 Hz DBS.

Stimulation at 130 Hz, as typically used to treat Parkinson's disease, was applied to all subjects (19 STN). However, as the time interval between pulses (7.7 ms) can be insufficient to reveal the resonant morphology of ERNA (Sinclair et al., 2018), stimulation was temporally patterned to allow multiple peaks to be observed. Two patterns were used: 1) applying a burst of ten 130 Hz pulses every second (Fig. 1B), and 2) omitting one pulse every second in otherwise continuous 130 Hz DBS (Fig. 1C). Stimulation with omitted pulses was expected to have comparable therapeutic efficacy to clinical 130 Hz DBS, as the total number of pulses delivered over time was reduced by only 0.77%, and is hereafter referred to as 'clinical' DBS. In contrast, the burst pattern was anticipated to have minimal therapeutic effects as only 7.7% of the pulses were delivered, making it a useful 'probe' stimulus for investigating ERNA during the pre- and post-DBS conditions.

Continuous 20 Hz stimulation was applied to a subset of six subjects (12 STN), in order to observe ERNA in response to a stimulus where the time period between individual pulses (50 ms) is greater than the presumed duration of the evoked response. STN DBS at 20 Hz has previously been demonstrated to have either minimal therapeutic effects or to mildly degrade motor performance (Chen et al., 2011; Chen et al., 2007).

First, 60s of probe stimulation was applied to the STN of one hemisphere in order to measure pre-DBS ERNA in the absence of therapy. Clinical stimulation was then applied with progressively increasing current amplitude (0.67, 1, 1.5, 2.25 and 3.38 mA). Each stimulation level was applied for 60s, except for 2.25 mA which was applied for 90s to allow time for therapeutic efficacy assessments as detailed below. Current amplitude was ramped up from the previous level over 1–2 s between conditions. Immediately after the 3.38 mA condition, 60s of probe stimulation was applied in order to observe any post-DBS washout effects. This process was then repeated for the STN in the other hemisphere. When used, 20 Hz DBS was then applied to the first hemisphere for 90s at 2.25 mA and subsequently to the second hemisphere.

The therapeutic efficacy of stimulation was assessed by rating limb bradykinesia and rigidity according to a modified version of the Unified Parkinson's Disease Rating Scale (UPDRS; items 22 and 23) before any stimulation was applied and between 60–90s of the 2.25 mA 130 Hz and 20 Hz conditions. Due to the coarse quantization of the UPDRS scale, each rating level was subdivided into 0.5 increments to provide a finer resolution. Such subdivision has been used in previous studies (Kwon et al., 2014; Prochazka et al., 1997). As rigidity and bradykinesia were the predominant symptoms across the cohort (Table 1), tremor was not assessed. The subject and the clinician performing assessments were blinded to the stimulation being applied.

As intraoperative time constraints precluded clinical assessments during each condition, spontaneous activity in the beta-band (13-30 Hz) was also used as an indicative measure of DBS therapeutic efficacy. Excessive synchronization of oscillations within the beta band has been strongly implicated in the pathophysiology of Parkinson's disease (Brown, 2003; Hammond et al., 2007) and its suppression has been correlated with improvement in bradykinesia and rigidity (Kühn et al., 2008; Kühn et al., 2009; Little and Brown, 2012).

The bursting pattern of probe stimulation also enabled analysis of spontaneous activity in the HFO band (200-400 Hz). By segmenting data to only include activity between bursts, epochs were obtained that were free of stimulation artefacts that would otherwise corrupt the HFO band.

Stimulation was delivered through the electrode targeting dorsal STN (E2, Fig. 1A), the region where DBS is reported to be most effective for Parkinson's disease (Herzog et al., 2004), using a highly configurable neurostimulator (Slater et al., 2015). Stimuli comprised symmetric constant-current biphasic pulses (60 μs per phase, negative phase first), to minimize the duration of stimulus artefacts that would otherwise corrupt ERNA. ERNA and local field potentials were recorded using a biosignal amplifier (g.USBamp, g.tec medical engineering GmbH, Schiedlberg, Austria) with a 38.4 kHz sampling rate. Adhesive Ag-AgCl electrodes were attached to each subject's shoulders for use as the amplifier reference and as a stimulation return electrode, respectively. A set of relays controlled by the neurostimulator was used to connect each electrode to either the neurostimulator or the amplifier. All electrodes were connected to the amplifier throughout the experiment, with the stimulating electrode (E2) temporarily switched to the neurostimulator to facilitate stimulus delivery. Monopolar recordings referenced to the Ag-AgCl reference electrode on the shoulder were obtained from all electrodes. Recordings were subsequently re-referenced to a bipolar configuration (E1-E3, Fig. 1A) across the stimulation electrode to be consistent with established methods for analyzing spontaneous beta-band activity (Little et al., 2013; Rossi et al., 2007)

2.3. Signal processing

Signal processing was performed using MATLAB (Mathworks, Massachusetts, USA). Recordings were then zero-phase forward-reverse filtered using a 2nd-order Butterworth high-pass filter (f_c = 2 Hz).

ERNA analysis involved first applying a 21-point centered moving average filter. A decaying exponential model was then fitted to and subtracted from each response to remove amplifier-settling baseline trends. The subtraction of exponential baseline trends did not affect the decaying oscillation morphology of ERNA. Peaks and troughs in the ERNA response were then found using the MATLAB 'findpeaks' function, which identifies local maxima as being greater than their neighboring samples according to user-defined criteria (MathWorks, 2019) (ERNA criteria: MinPeakWidth = 0.5 ms, MinPeakProminence = 10 μV). Spurious ERNA responses were rejected from further analysis if there were fewer than 2 peaks and 2 troughs, and by applying thresholds to the mean (> 1 ms) and standard deviation (< 1 ms) of the difference in latency between the first 2 peaks and 2 troughs (< 1.1% responses rejected). ERNA frequency was calculated as the inverse of the time difference between the first and second peak. ERNA amplitude was calculated as the difference between the first peak and the subsequent trough.

Spontaneous beta-band activity during clinical stimulation was processed using short-time Fourier transforms of 1 s Blackman-Harris windowed epochs temporally aligned to begin on each omitted pulse. 'Relative beta' was calculated as the RMS amplitude within the 13-30 Hz band divided by that within 5-45 Hz. The use of a relative measure accentuated changes in beta-band peaks over variation in wideband activity and is an established technique for adjusting for

differences in the magnitude of activity across subjects (Bronzino, 1999).

Spontaneous beta and HFO activity during probe stimulation were processed using 750 ms epochs extracted from between bursts to avoid stimulation artefacts in the HFO band. Beta activity was analyzed using short-time Fourier transforms, as above. As HFO activity was generally characterized by a broadband peak in frequency, Thomson's multi-taper spectral estimates (20 tapers) were used. HFO frequency and amplitude were quantified for analysis. HFO frequency was defined as the frequency of the largest peak occurring between 150 and 450 Hz in the estimated spectrum for each epoch, as determined using the MATLAB 'findpeaks' function (HFO criteria: MinPeakWidth = 26.6 Hz). HFO amplitude was defined as the RMS amplitude between 150 and 450 Hz divided by that between 150 and 750 Hz. A relative measure was used for HFO amplitude in order to adjust for interpatient differences and to be consistent with beta analyses. The frequency range of 150-450 Hz, which is ± 50 Hz wider than the nominal 200-400 Hz HFO band, was used for both frequency and amplitude assessments to ensure that the very broad HFO peaks were adequately captured.

Epochs corrupted by movement artefacts and other spurious signals were rejecting by thresholding the amplitude of the beta band and the 4-12 Hz, 37-47 Hz or 53-63 Hz sub-bands at 1.5 times their interquartile range across each stimulation condition (< 1.1% of epochs rejected). Five entire stimulation blocks were also rejected from spontaneous beta analysis due to excessive non-physiological electrical noise (PD03 right 1.5 mA, PD12 left 1–3.375 mA).

As it is well established that DBS therapy has a 'wash-in' time (Temperli et al., 2003), when comparing data across clinical DBS levels, averages across the 45–60s period were used for analysis, with the first 45 s treated as wash-in time for effects to approach steady-state values. When comparing data within conditions, averages across 15 s non-overlapping blocks were used.

Statistical analyses were performed using SigmaPlot (Systat, California, USA) using a significance level of $p < .05$. As data tended to be non-normal (Shapiro-Wilk normality test) non-parametric tests were used where appropriate. The tests applied are specified where relevant in the results.

3. Results

ERNA was consistently observed in all 19 STN tested.

3.1. Clinical DBS at 130 Hz modulates ERNA

Progressively increasing the amplitude of clinical 130 Hz DBS modulated the morphology of ERNA. Fig. 2A shows the ERNA recorded around each omitted pulse for one STN, where clear peaks can be seen to gradually vary within, and across, stimulation conditions. Generally, the second peak (typically ~7 ms initially) and subsequent peaks were observed to asymptotically increase in latency and spread further apart, indicating a decrease in the frequency of the evoked activity. In many cases, e.g. Fig. 2A, the latency of the first peak (typically ~4 ms initially) also increased, although this was not consistent across all STN.

ERNA frequency varied significantly with stimulation amplitude (Friedman Repeated Measures ANOVA on Ranks, $\chi^2(4) = 59.75$, $p < .001$). Tukey post hoc comparisons indicated that ERNA frequency initially decreased with increasing DBS amplitude and plateaued around 2.25 mA (Fig. 2C). The median frequency was 256 Hz at 3.38 mA, approximately twice the stimulation rate of 130 Hz. ERNA amplitude also varied significantly with stimulation amplitude (Friedman, $\chi^2(4) = 41.31$, $p < .001$). Tukey post hoc comparisons indicated that ERNA amplitude initially increased with DBS amplitude and then plateaued at levels above 1.5 mA (Fig. 2D).

In contrast, 20 Hz stimulation did not modulate ERNA. While 20 Hz DBS elicited multi-peaked responses (Fig. 3A), it did not vary across the 90s period (Fig. 3B). For the 12 STN tested, ERNA frequency and amplitude averaged across 15 s non-overlapping blocks were not significantly different over time (20 Hz ERNA frequency: range: 271-458 Hz, median: 326 Hz; Friedman, $\chi^2(5) = 3$, $p = .7$; 20 Hz ERNA amplitude: range: 36-413 μV, median: 131 μV; Friedman, $\chi^2(5) = 5.67$, $p = .34$). In comparison, for 130 Hz clinical DBS applied to the same subset of STN, ERNA frequency and amplitude averaged over 15 s non-overlapping blocks varied significantly over time, independent of the effects of different DBS amplitudes (130 Hz ERNA frequency: 2-way Repeated Measures ANOVA, time: $F(3,239) = 75.02$, $p < .001$, DBS amplitude: $F(4,239) = 30.55$, $p < .001$, time x DBS amplitude: $F(12,239) = 1.02$, $p = .43$; 130 Hz ERNA amplitude: 2-way Repeated Measures ANOVA, time: $F(3,239) = 3.97$, $p = .016$, DBS amplitude: $F(4,239) = 11.06$, $p < .001$, time x DBS amplitude: $F(12,239) = 0.77$, $p = .68$).

3.2. ERNA modulation coincides with therapeutic effect

Bradykinesia and rigidity UPDRS scores improved significantly across the cohort during clinical 2.25 mA 130 Hz stimulation (Wilcoxon Signed Rank test, bradykinesia: $Z = -3.62$, $p < .001$, rigidity: $Z = -3.70$, $p < .001$, Supplementary Table 1), indicating that DBS was generally therapeutic at 2.25 mA. Clinical signs were not significantly affected by 20 Hz DBS (Wilcoxon, bradykinesia: $Z = 1.41$, $p = .22$, rigidity: $Z = -1.61$, $p = .15$).

Relative beta amplitude during clinical 130 Hz DBS was also found to vary significantly with stimulation amplitude (Friedman, $\chi^2(4) = 30.07$, $p < .001$). Post hoc tests (Tukey) showed significant suppression at 3.38 mA compared to 0.67, 1 and 1.5 mA and at 2.25 mA compared to 0.67 mA (Fig. 2E). As beta suppression has been shown to correlate with improvement in motor signs (Kühn et al., 2008; Kühn et al., 2009; Little and Brown, 2012) this further supports that stimulation was therapeutically effective at approximately 2.25 mA and above.

Using average values from 15 s non-overlapping blocks across each condition, ERNA frequency was found to be significantly correlated with relative beta (Fig. 2F, Spearman rank order correlation, $\rho = 0.58$, $n = 360$, $p < .001$). ERNA amplitude was not significantly correlated with relative beta (Spearman, $\rho = 0.0625$, $n = 360$, $p = .237$), possibly due to the sigmoidal-like variation in ERNA amplitude with stimulation amplitude.

3.3. ERNA modulation washes out after DBS

Using probe stimulation (bursts of 10 pulses) ERNA modulation was found to washout after cessation of therapeutic 130 Hz DBS (e.g. Fig. 4A). Post-DBS, ERNA peaks initially occurred at longer latencies before gradually returning towards the pre-DBS state measured before clinical stimulation was applied. Additionally, ERNA was generally stable pre-DBS, indicating that the modulatory effects of probe stimulation were minimal and that the washout effects observed post-DBS can be attributed to underlying changes in STN neural state.

Compared to the last 15 s of the pre-DBS condition, ERNA frequency was found to be significantly decreased post-DBS (Friedman, $\chi^2(4) = 70.23$, $p < .001$) until the final 45–60s block (Tukey post hoc, $p = .73$) (Fig. 4D). ERNA amplitude also significantly varied (Friedman, $\chi^2(4) = 31.37$, $p < .001$), with differences between post-DBS time points indicating a washout of amplitude suppression caused by therapeutic stimulation (Fig. 4E).

Beta activity also varied pre- and post-DBS (e.g. Fig. 4B). Consistent with previous reports (Bronte-Stewart et al., 2009; Kühn et al., 2008), relative beta was significantly decreased post-DBS (Friedman, $\chi^2(4) = 22.95$, $p < .001$, Tukey post hoc) and washed out to approach pre-DBS levels after 30s (Fig. 4F). Consistent with the clinical DBS results, ERNA frequency was significantly correlated with relative beta pre- and post-DBS (Spearman, $\rho = 0.48$, $n = 152$, $p < .001$). ERNA amplitude was also correlated with relative beta (Spearman, $\rho = 0.31$,

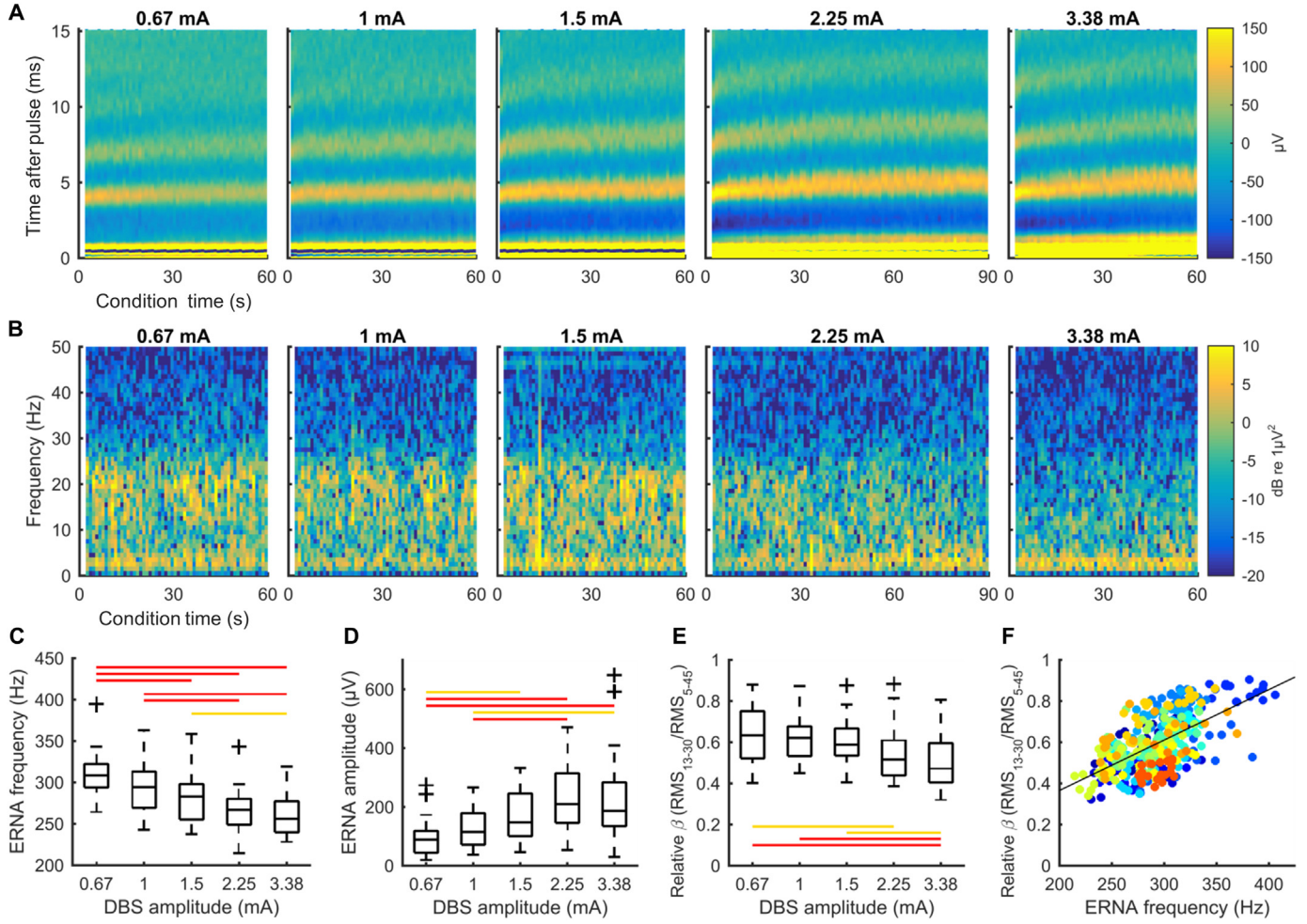

Fig. 2. Clinical 130 Hz DBS modulates ERNA. (A) ERNA recorded from the left STN of a Parkinson's disease subject during clinical stimulation as DBS current amplitude (indicated at the top of each subplot) is increased. Plots comprise each ERNA response measured when a pulse was omitted, with color representing amplitude (μV) and ERNA peaks appearing as yellow. The y-axis corresponds to the time window between pulses in which ERNA can be measured (Fig. 1C) and the x-axis corresponds to the overall stimulation time for each condition. (B) Spectrograms showing beta activity (13-30 Hz) during clinical stimulation, with color representing power (dB). (C) ERNA frequency vs DBS amplitude across all 19 STN tested (average value across the 45–60s period of each condition used for ERNA frequencies; red bars: $p \leq .001$; yellow bars: $p < .05$; Box: 25-75th percentile; central line: median; whiskers: range excluding outliers; +: outliers extending beyond the 25th–75th percentiles by 1.5 times the interquartile range). (D) ERNA amplitude vs DBS amplitude. (E) Relative beta ($RMS_{13\text{-}30}$ Hz/$RMS_{5\text{-}45}$ Hz) vs DBS amplitude. (F) Relative beta correlated with ERNA frequency ($\rho = 0.58$, $p < .001$). Colors represent different STN tested. (For interpretation of the references to color in this figure legend, the reader is referred to the web version of this article.)

$n = 152$, $p < .001$), suggesting it too may have clinical and mechanistic relevance.

3.4. Therapeutic 130 Hz DBS modulates HFO

The bursting pattern of probe stimulation allowed analysis of spontaneous activity in the HFO band (200-400 Hz) (e.g. Fig. 4C), which overlaps with the range of observed ERNA frequencies.

HFO peak frequency was found to be significantly decreased post-DBS (Friedman, $\chi^2(4) = 33.1$, $p < .001$), except for the final 45–60s block (Tukey post hoc, $p = .077$) (Fig. 4G). This washout trend matches that for ERNA frequency, albeit at frequencies around 80 Hz lower, and a significant correlation was found between them (Spearman, $\rho = 0.58$, $n = 152$, $p < .001$). The median HFO peak frequency immediately post-DBS was 256 Hz, approximately two times the stimulation rate and matching the median ERNA frequency of the therapeutic 3.38 mA condition, suggesting HFO activity may occur at the same frequency as ERNA during clinical stimulation. No significant differences were found in HFO peak amplitude (Friedman, $\chi^2(4) = 3.75$, $p = .44$), although it is possible that the very small amplitude of HFO peaks resulted in any modulatory effects being obscured by noise in the recordings.

4. Discussion

This study demonstrates that DBS evokes a resonant neural response, ERNA, in the STN of patients with Parkinson's disease that is modulated by increasing clinical 130 Hz stimulation to therapeutic levels. Furthermore, modulation of frequency and amplitude of ERNA coincides with therapeutic benefit, suppression of spontaneous beta band activity, and a decrease in spontaneous HFO frequency to around twice the stimulation rate. In contrast, non-therapeutic 20 Hz DBS elicited ERNA but did not affect it over time. These findings have implications for understanding DBS mechanisms and indicate that ERNA has key attributes of a dynamic feedback signal for optimizing therapy.

Before further discussion, several limitations need consideration. Firstly, the sample size of 19 STN from 10 subjects is modest. However, the presence and modulation of ERNA was observed in all STN tested. Secondly, this study was performed intraoperatively. This limited the time available and consequently subjects were only studied off medication and clinical assessments were only performed at one stimulation

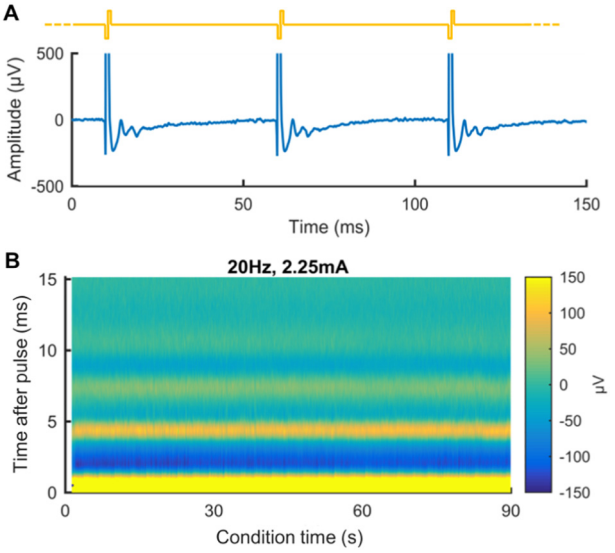

Fig. 3. 20 Hz DBS elicits, but does not modulate, ERNA. (A) ERNA elicited by 2.25 mA 20 Hz DBS applied to the same STN as in Fig. 2 (yellow trace: stimulation waveform). (B) 20 Hz ERNA over 90s for same STN. Plot comprises each ERNA response measured after each pulse, with color representing amplitude (μV) and ERNA peaks appearing as yellow. The y-axis corresponds to the time after each pulse and the x-axis corresponds to the overall stimulation time. (For interpretation of the references to color in this figure legend, the reader is referred to the web version of this article.)

level. Time limitations also precluded washout periods between conditions and an initial assessment of each subject's maximum tolerable stimulation level. Consequently, DBS level was progressively increased and analyses focused on the 45–60s period of each condition to allow for any potential carry-over effects. Intraoperative time limitations also prevented 20 Hz DBS being tested at more than one stimulation amplitude. It is possible that 20 Hz DBS did not modulate ERNA as the total power delivered over time is substantially reduced by the low stimulation rate, which could be investigated in future studies.

4.1. What is ERNA?

Several potential neural mechanisms could underlie the generation of ERNA. For instance, ERNA could arise entirely within the STN due to synchronized periods of excitation and inhibition following each DBS pulse. Notably, the ERNA peaks coincide with the time course of firing rate recovery within the STN of Parkinsonian non-human primates following DBS pulses (Meissner et al., 2005).

ERNA could also reflect activity elicited in other structures that is propagated to the STN. Antidromic activation of STN afferents, a proposed mechanism of action of DBS (Gradinaru et al., 2009), has been shown to elicit multiphasic activity in the cortex (Ashby et al., 2001; Baker et al., 2002; Kuriakose et al., 2009; Li et al., 2007). Ashby et al. (Ashby et al., 2001) further reported a progressive increase in cortical evoked potential amplitude over a burst of eight pulses delivered at 200 Hz, comparable to that observed with ERNA during burst probe DBS (e.g. Fig. 1B). Multiphasic evoked potentials have also been reported with pallidal (Tisch et al., 2008) and thalamic DBS (Walker et al., 2012), further implicating cortical activity in DBS mechanisms. ERNA may therefore reflect cortical activity being propagated to the STN.

Alternatively or additionally, ERNA could arise from activity propagating around loops re-entrant to, or within, the STN, with ERNA morphology dependent on the resonant frequency of the neural circuits. The STN is part of the highly interconnected cortico-basal ganglia-thalamo-cortical network (Herrington et al., 2015; McIntyre and Hahn, 2010; Montgomery and Gale, 2008; Wichmann and DeLong, 2016), which seems well suited to produce resonant activity. Indeed, the network has been proposed to operate as a system of loosely coupled

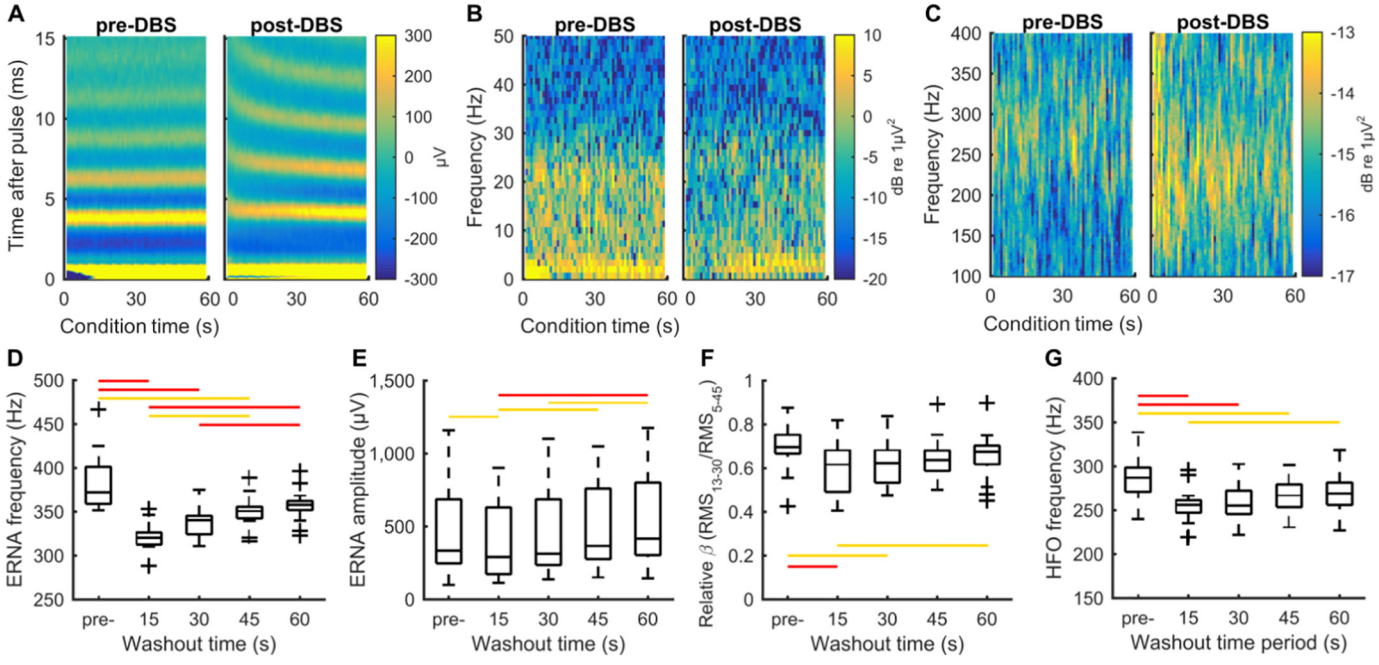

Fig. 4. Washout effects following cessation of therapeutic DBS. (A) ERNA during non-therapeutic probe stimulation immediately pre- and post- 5.5 min of clinical stimulation for same STN as in Figs. 2 and 3. Here, ERNA has been recorded after the last pulse of each probe burst, with color representing ERNA amplitude (μV) and peaks appearing as yellow. The y-axis corresponds to time after the last pulse of each burst and the x-axis corresponds to the overall stimulation time for each condition. (B) Spectrograms showing beta activity (13-30 Hz) during probe stimulation, with color representing power (dB). (C) Multi-taper spectral density estimates of high frequency oscillations (HFO) during probe stimulation, with color representing power (dB). (D) ERNA frequency washout over consecutive 15 s periods post-DBS and in the last 15 s pre-DBS. Red bars: $p \leq .001$, yellow bars: $p < .05$. (E) ERNA amplitude washout. (F) Relative beta washout. (G) HFO frequency washout. (For interpretation of the references to color in this figure legend, the reader is referred to the web version of this article.)

oscillatory feedback loops whose dynamics can be modulated by DBS (Leblois et al., 2006; Montgomery and Gale, 2008; Montgomery Jr, 2004; Montgomery Jr, 2016; Tass, 1999). For instance, the STN is reciprocally connected to the globus pallidus externa, which has been proposed to form a central pacemaker circuit that supports oscillatory activity (Bevan et al., 2002; Mastro and Gittis, 2015). Loop delays of around 2-4 ms could produce recurring activity in the range 250-500 Hz, as seen with ERNA.

4.2. ERNA and spontaneous HFO activity

If ERNA arises from resonant network activity, it can be speculated that spontaneous neural activity could also be propagating within the same or related circuits. Intriguingly, ERNA and HFO appear closely related, occupying similar frequency bands and both being modulated to around twice the 130 Hz stimulation rate. However, pre- and post-DBS ERNA frequencies measured using burst probe stimulation were approximately 80 Hz higher than HFO frequencies. This may be due to transient start-up effects at the onset of stimulation, e.g. Fig. 1B, resulting in an overestimate of the underlying neural state frequency. Importantly, HFO frequencies in the first 15 s post-DBS (219-296 Hz, median: 256 Hz) were congruent with ERNA frequencies during the preceding 3.38 mA clinical DBS condition (228–319 Hz, median: 256 Hz), suggesting they occur at the same or very similar frequencies and may be mechanistically related. For example, ERNA and HFO could arise from the same neural networks, or from separate networks that are brought into a coherent oscillatory state to facilitate neural communication and function (Fries, 2005), or both.

HFO activity has been found to be modulated by movement and medication (Foffani et al., 2003; López-Azcárate et al., 2010; Özkurt et al., 2011); however, the neural mechanisms underlying its generation are largely unknown (Wang et al., 2014; Yang et al., 2014). Yang et al. (Yang et al., 2014) proposed that desynchronized neural clusters firing out of phase with each other could produce HFO activity at frequencies higher than individual firing rates. Such an effect could also result from time delays between interconnected neural clusters producing phase shifted versions of a neural spike train. Delays could occur between clusters in the vicinity of the recording electrode, or as a result of network loops re-entrant to, or within, the STN, as proposed above.

4.3. Modulatory mechanisms of DBS

Several possible mechanisms could account for the modulation of ERNA and HFO. For instance, DBS may provide a forcing function (Montgomery Jr, 2004) that drives the underlying circuits to a different oscillatory state. Such entrainment could result from DBS producing an “information lesion” by regularly rendering neurons refractory and eliciting antidromic activation that creates an axonal blockade (Grill et al., 2004). Alternatively, DBS may cause network desynchronization that resets it to a different state (Tass, 1999).

Notably, the median frequency of both ERNA during 3.38 mA clinical stimulation and HFO immediately post-DBS was 256 Hz, approximately two times the stimulation rate. The wide range of ERNA and HFO frequencies across individuals (~100 Hz) indicates that they are not simply being driven to a harmonic of the stimulation rate, but rather suggests that each individual may have an intrinsic oscillatory state around 220–320 Hz that supports normal function. That 130 Hz stimulation is typically effective in most patients fits with the understanding that stimulation at a submultiple of a system's intrinsic frequency is effective at driving the system towards that frequency. Thus, ERNA frequency may provide a method for identifying the optimal stimulation rate for each individual patient.

Modulation could also occur as a result of interactions between resonant activity and subsequent DBS pulses (Montgomery and Gale, 2008). For instance, if a subsequent DBS pulse occurs within the peak or trough of ERNA from the preceding pulse, it may reinforce or suppress the oscillation. This may explain why 20 Hz DBS did not modulate ERNA, as the evoked resonance seemed to decay between successive pulses, eliminating the likelihood of inter-pulse interactions.

Resonant changes could also reflect a shift in dominance between multiple competing feedback loops (Leblois et al., 2006). Multiple HFO peaks, one around 250-300 Hz and another around 300-350 Hz, have been previously reported, with the power ratio shifting to the higher frequency with levodopa administration (Özkurt et al., 2011). Such peaks could stem from separate networks and, through mechanisms such as preferential blockade of certain axons (García et al., 2013), DBS could shift the dominance of one loop over the other. Such effects could also account for the higher frequency of probe-ERNA, with the burst patterning preferentially activating a faster loop.

The shift in HFO power to higher frequencies with levodopa therapy (Foffani et al., 2003; López-Azcárate et al., 2010; Özkurt et al., 2011; van Wijk et al., 2016), reported in some but not all patients (López-Azcárate et al., 2010), is contrary to the decrease in HFO peak frequency found here after therapeutic DBS. While the empirical effects of DBS on HFO activity are yet to be comprehensively established, opposing frequency shift directions suggests that levodopa and DBS may have different therapeutic mechanisms of action.

4.4. Practical utility of ERNA

ERNA's relatively large amplitude (20-681$\mu V_{p\text{-}p}$, median 146$\mu V_{p\text{-}p}$), is orders of magnitude greater than beta (0.9–12.5μV_{RMS}, median: 2.2μV_{RMS}), and implantable technology capable of measuring such evoked activity has already been implemented in other neural prosthetic applications (Shallop et al., 1999). The robustness of ERNA and its distinct and gradually modulated morphology (Fig. 2A and 4A) also contrast with the inherent variability in beta-band activity across patients (Little and Brown, 2012) and its noisy, bursting on-off nature (Tinkhauser et al., 2017) (Fig. 2B and 4B).

Significant changes with therapeutically-effective DBS and correlation with spontaneous neural activity features known to reflect motor state indicates that ERNA modulation is occurring at the same time as clinically relevant changes in the underlying neural circuits. Thus, ERNA is a potentially useful signal for optimizing DBS therapy.

Both ERNA frequency and amplitude were modulated by DBS, suggesting each may have practical utility. However, ERNA amplitude was found to increase and plateau with increasing clinical DBS level (Fig. 2D), yet was contrarily found to be reduced post-DBS compared to baseline levels (Fig. 4E). As the probe stimulus used pre- and post-DBS was constant, the reduction in ERNA amplitude can be directly attributed to changes in STN neural state. Therefore, while ERNA amplitude contains clinically relevant information, it can be obscured by effects related to changes in stimulus intensity, such as increasing spread of activation and saturation of neural firing.

Different aspects of ERNA, including parameters not explored here such as latency and decay-rate, may therefore be suitable for different clinical applications. ERNA amplitude has shown potential for identifying the optimal sites for stimulation (Sinclair et al., 2018), and therefore has utility for electrode implantation guidance and configuration. ERNA frequency, less likely to be confounded by stimulus level effects, has potential as a feedback signal for objectively comparing and selecting stimulation settings, and for implementing DBS strategies that automatically adapt to real-time patient needs. Such enhancements could enable a paradigm shift in the clinical application of DBS that could substantially improve outcomes by tailoring therapy to each patient.

5. Conclusions

This study has shown that DBS in the vicinity of the STN evokes a resonant neural response, ERNA, that is modulated by therapeutic 130 Hz stimulation. ERNA modulation correlated with suppression of

spontaneous beta-band activity and with changes in spontaneous high frequency oscillations occurring in a similar frequency band. These results suggest that therapeutic DBS modulates the natural oscillation frequency of basal ganglia circuits, which is reflected in changes in high-frequency spontaneous neural activity. Thus, ERNA has potential as a tool for providing insight into brain network function and has key attributes of a dynamic feedback signal for optimizing therapy.

Funding sources

This work was supported by the Colonial Foundation, St Vincent's Hospital Research Endowment Fund, and the National Health and Medical Research Council [project grant #1103238]. The Bionics Institute acknowledges the support it receives from the Victorian Government through its operational infrastructure program. N.C.S. is supported through an Australian Government Research Training Program Scholarship. P.B. is supported by the Medical Research Council of Great Britain. W.T is supported by Lions International and the National Health and Medical Research Council.

Declaration of Competing Interest

None.

Acknowledgements

None.

Appendix A. Supplementary data

Supplementary data to this article can be found online at https://doi.org/10.1016/j.nbd.2019.104522.

References

Arlotti, M., et al., 2016. An external portable device for adaptive deep brain stimulation (aDBS) clinical research in advanced Parkinson's disease. Med. Eng. Phys. 38, 498–505.
Ashby, P., et al., 2001. Potentials recorded at the scalp by stimulation near the human subthalamic nucleus. Clin. Neurophysiol. 112, 431–437.
Baker, K.B., et al., 2002. Subthalamic nucleus deep brain stimulus evoked potentials: physiological and therapeutic implications. Mov. Disord. 17, 969–983.
Bevan, M.D., et al., 2002. Move to the rhythm: oscillations in the subthalamic nucleus–external globus pallidus network. Trends Neurosci. 25, 525–531.
Bronte-Stewart, H., et al., 2009. The STN beta-band profile in Parkinson's disease is stationary and shows prolonged attenuation after deep brain stimulation. Exp. Neurol. 215, 20–28.
Bronzino, J.D., 1999. Biomedical Engineering Handbook. CRC Press.
Brown, P., 2003. Oscillatory nature of human basal ganglia activity: relationship to the pathophysiology of Parkinson's disease. Mov. Disord. 18, 357–363.
Chen, C.C., et al., 2007. Excessive synchronization of basal ganglia neurons at 20 Hz slows movement in Parkinson's disease. Exp. Neurol. 205, 214–221.
Chen, C.C., et al., 2011. Stimulation of the subthalamic region at 20 Hz slows the development of grip force in Parkinson's disease. Exp. Neurol. 231, 91–96.
de Hemptinne, C., et al., 2013. Exaggerated phase-amplitude coupling in the primary motor cortex in Parkinson disease. Proc. Natl. Acad. Sci. U. S. A. 110, 4780–4785.
Diamond, A., Jankovic, J., 2005. The effect of deep brain stimulation on quality of life in movement disorders. Journal of Neurology. Neurosurg. Psychiatr. 76, 1188–1193.
Foffani, G., et al., 2003. 300-Hz subthalamic oscillations in Parkinson's disease. Brain. 126, 2153–2163.
Fries, P., 2005. A mechanism for cognitive dynamics: neuronal communication through neuronal coherence. Trends Cogn. Sci. 9, 474–480.
García, M.R., et al., 2013. A slow axon antidromic blockade hypothesis for tremor reduction via deep brain stimulation. PLoS One 8, e73456.
Gradinaru, V., et al., 2009. Optical deconstruction of parkinsonian neural circuitry. Science. 324, 354–359.
Grill, W.M., et al., 2004. Deep brain stimulation creates an informational lesion of the stimulated nucleus. Neuroreport. 15, 1137–1140.
Hammond, C., et al., 2007. Pathological synchronization in Parkinson's disease: networks, models and treatments. Trends Neurosci. 30, 357–364.
Herrington, T.M., et al., 2015. Mechanisms of deep brain stimulation. J. Neurophysiol. 115, 19–38.
Herzog, J., et al., 2004. Most effective stimulation site in subthalamic deep brain stimulation for Parkinson's disease. Mov. Disord. 19, 1050–1054.
Kühn, A.A., et al., 2008. High-frequency stimulation of the subthalamic nucleus suppresses oscillatory β activity in patients with Parkinson's disease in parallel with improvement in motor performance. J. Neurosci. 28, 6165–6173.
Kühn, A.A., et al., 2009. Pathological synchronisation in the subthalamic nucleus of patients with Parkinson's disease relates to both bradykinesia and rigidity. Exp. Neurol. 215, 380–387.
Kuriakose, R., et al., 2009. The nature and time course of cortical activation following subthalamic stimulation in Parkinson's disease. Cereb. Cortex 20, 1926–1936.
Kwon, Y., et al., 2014. Quantitative evaluation of parkinsonian rigidity during intra-operative deep brain stimulation. Biomed. Mater. Eng. 24, 2273–2281.
Leblois, A., et al., 2006. Competition between feedback loops underlies normal and pathological dynamics in the basal ganglia. J. Neurosci. 26, 3567–3583.
Li, S., et al., 2007. Resonant antidromic cortical circuit activation as a consequence of high-frequency subthalamic deep-brain stimulation. J. Neurophysiol. 98, 3525–3537.
Little, S., Brown, P., 2012. What brain signals are suitable for feedback control of deep brain stimulation in Parkinson's disease? Ann. N. Y. Acad. Sci. 1265, 9–24.
Little, S., et al., 2013. Adaptive deep brain stimulation in advanced Parkinson disease. Ann. Neurol. 74, 449–457.
López-Azcárate, J., et al., 2010. Coupling between beta and high-frequency activity in the human subthalamic nucleus may be a pathophysiological mechanism in Parkinson's disease. J. Neurosci. 30, 6667–6677.
Marsden, C., et al., 1982. Fluctuations of Disability in Parkinson's Disease: Clinical Aspects. Movement Disorders. 198. Butterworth, London, pp. 96–122.
Mastro, K.J., Gittis, A.H., 2015. Striking the right balance: cortical modulation of the subthalamic nucleus-globus pallidus circuit. Neuron. 85, 233–235.
MathWorks, findpeaks Accessed: 22nd February 2019. https://au.mathworks.com/help/signal/ref/findpeaks.html.
McIntyre, C.C., Hahn, P.J., 2010. Network perspectives on the mechanisms of deep brain stimulation. Neurobiol. Dis. 38, 329–337.
Meissner, W., et al., 2005. Subthalamic high frequency stimulation resets subthalamic firing and reduces abnormal oscillations. Brain. 128, 2372–2382.
Montgomery, E.B., Gale, J.T., 2008. Mechanisms of action of deep brain stimulation (DBS). Neurosci. Biobehav. Rev. 32, 388–407.
Montgomery Jr., E.B., 2004. Dynamically coupled, high-frequency reentrant, non-linear oscillators embedded in scale-free basal ganglia-thalamic-cortical networks mediating function and deep brain stimulation effects. Nonlinear Stud. 11.
Montgomery Jr., E.B., 2016. Deep Brain Stimulation Programming: Mechanisms, Principles, and Practice. Oxford University Press.
Neumann, W.J., et al., 2016. Deep brain recordings using an implanted pulse generator in Parkinson's disease. Neuromodulation Technol. Neural Interface. 19, 20–24.
Okun, M.S., 2012. Deep-brain stimulation for Parkinson's disease. N. Engl. J. Med. 367, 1529–1538.
Özkurt, T.E., et al., 2011. High frequency oscillations in the subthalamic nucleus: a neurophysiological marker of the motor state in Parkinson's disease. Exp. Neurol. 229, 324–331.
Priori, A., et al., 2013. Adaptive deep brain stimulation (aDBS) controlled by local field potential oscillations. Exp. Neurol. 245, 77–86.
Prochazka, A., et al., 1997. Measurement of rigidity in Parkinson's disease. Mov. Disord. 12, 24–32.
Rosin, B., et al., 2011. Closed-loop deep brain stimulation is superior in ameliorating parkinsonism. Neuron. 72, 370–384.
Rossi, L., et al., 2007. An electronic device for artefact suppression in human local field potential recordings during deep brain stimulation. J. Neural Eng. 4, 96.
Shallop, J.K., et al., 1999. Neural response telemetry with the nucleus CI24M cochlear implant. Laryngoscope 109, 1755–1759.
Sinclair, N.C., et al., 2018. Subthalamic nucleus deep brain stimulation evokes resonant neural activity. Ann. Neurol. 83, 1027–1031.
Slater, K.D., et al., 2015. neuroBi: a highly configurable neurostimulator for a retinal prosthesis and other applications. IEEE J. Transl. Eng. Health Med. 3, 1–11.
Stanslaski, S., et al., 2012. Design and validation of a fully implantable, chronic, closed-loop neuromodulation device with concurrent sensing and stimulation. IEEE Trans. Neural Syst. Rehabil. Eng. 20, 410–421.
Swann, N.C., et al., 2018. Adaptive deep brain stimulation for Parkinson's disease using motor cortex sensing. J. Neural Eng. 15, 046006.
Tass, P.A., 1999. Phase Resetting in Medicine and Biology: Stochastic Modelling and Data Analysis. Springer Science & Business Media.
Temperli, P., et al., 2003. How do parkinsonian signs return after discontinuation of subthalamic DBS? Neurology. 60, 78–81.
Tinkhauser, G., et al., 2017. The modulatory effect of adaptive deep brain stimulation on beta bursts in Parkinson's disease. Brain. 140, 1053–1067.
Tisch, S., et al., 2008. Cortical evoked potentials from pallidal stimulation in patients with primary generalized dystonia. Mov. Disord. 23, 265–273.
van Wijk, B.C., et al., 2016. Subthalamic nucleus phase–amplitude coupling correlates with motor impairment in Parkinson's disease. Clin. Neurophysiol. 127, 2010–2019.
Walker, H.C., et al., 2012. Short latency activation of cortex by clinically effective thalamic brain stimulation for tremor. Mov. Disord. 27, 1404–1412.
Wang, J., et al., 2014. High-frequency oscillations in Parkinson's disease: spatial distribution and clinical relevance. Mov. Disord. 29, 1265–1272.
Wichmann, T., DeLong, M.R., 2016. Deep brain stimulation for movement disorders of basal ganglia origin: restoring function or functionality? Neurotherapeutics. 13, 264–283.
Yang, A.I., et al., 2014. Beta-coupled high-frequency activity and beta-locked neuronal spiking in the subthalamic nucleus of Parkinson's disease. J. Neurosci. 34, 12816–12827.